

Accumulation of Microswimmers due to Their Collisions with a Surface

Guanglai Li and Jay X. Tang

Physics Department, Brown University, Providence RI 02912

In this letter we propose a kinematic model to show how collisions with a surface and rotational Brownian motion give rise to the accumulation of micro-swimmers near a surface. In this model, an elongated microswimmer invariably travels parallel to the surface after hitting it from any incident angle. It then swims away from the surface after some time, facilitated by rotational Brownian motion. Simulations based on this model reproduce the density distributions measured for the small bacteria *E. coli* and *Caulobacter crescentus*, as well as for the much larger bull spermatozoa swimming in confinement.

Swimming aids the function and development of microorganisms in many ways. For example, it enhances the formation of biofilms, which provide favorable microenvironments for bacteria to cope with environmental stresses [1]. Swimming also helps transport spermatozoa toward eggs for fertilization [2]. Interestingly, the number density of cells as a function of distance from a surface has been measured for *E. coli* [3] and bull spermatozoa [4], showing in both cases values much higher near the surface than far away. This near surface accumulation has mainly been attributed to a hydrodynamic attraction between the cells and the surface [4, 5]. Recently, Berke *et al.* [3] combined the effects of the hydrodynamic attraction and the translational Brownian motion of the cells to predict the distribution of *E. coli* as a function of distance. As noted by the authors [3], however, this interpretation is not applicable to cells within 10 μm from the surface, where most accumulation occurs.

In this letter we present a different account for the near surface accumulation. We ignore the hydrodynamic attraction but emphasize the role of the collision with a surface at low Reynolds number and rotational Brownian motion in a confined environment. We show that a typical microswimmer with an elongated shape will swim parallel to a surface after hitting it and therefore accumulate near the surface. Rotational Brownian motion [6] then relaxes the accumulation by randomly changing the swimming direction so that the cells have chances to swim away from the surface. In the extreme case of no rotational Brownian motion, all the cells would end up swimming in close proximity with the surface. In the opposite extreme of very fast rotational Brownian motion, the cells will quickly change to any possible swimming direction and subsequently would be found anywhere with equal probability. In reality, a microorganism randomly changes its swimming direction with a finite rotational diffusion constant, resulting in a distribution in between the two extremes, that is, more cells stay near the surface and fewer far away.

We used the bacterium *C. crescentus* strain CB15 SB3860, which is a CheR mutant of $\Delta pilin$ (YB375) and swims forward exclusively, to examine the details of near surface swimming. Swarmer cells of this mutant do not follow circular trajectories when swimming near surfaces [7]. The strains were synchronized with

the plate releasing method [7, 8] to obtain cultures with primarily swimming cells. The synchronized culture was sealed between a glass slide and a coverslip with vacuum grease for optical microscopy observation. Broken coverslip pieces were used as spacers so that the thickness of the microscopy sample is $\sim 200 \mu\text{m}$. A $20\times$ objective (Nikon Plan Apo, NA 0.75) was used on a Nikon E800 microscope to take 5 snap shots of swimming cells at 0.1 second intervals under darkfield mode using a CoolSnap CCD camera (Princeton Instruments) and MetaMorph software (Universal Imaging). The objective was focused on planes 5, 15, 25 μm , *etc.*, away from the surface and the cell number distribution was measured following the method of Berke *et al.* [3]. We noted that although this objective has a 1.4 μm depth of field, cells up to nearly 5 μm off the focal plane appeared as bright spots. Therefore the measured cell density was an average over a $\sim 10 \mu\text{m}$ thick layer.

The swimming speed and the rotational diffusion constant were obtained from the videos taken for cells over 50 μm away from both surfaces. The average swimming speed was $\sim 45 \mu\text{m/s}$. The rotational diffusion constant was measured from ~ 200 swimming trajectories. The swimming direction at moment t was taken as the direction from the position at t to the position at $t + 0.1$ s. With this definition the change in direction $\Delta\varphi$ over time interval Δt was obtained and the rotational diffusion constant D_r was calculated to be $0.12 \text{ rad}^2/\text{s}$, using the equation $\langle \Delta\varphi^2 \rangle = 2D_r\Delta t$.

With particular interest we examined 3-D trajectories as the cells approached and swam near a surface, until they took off. To do so, we focused the objective on the top surface and recorded the swimming trajectories. Example trajectories are shown in Fig. 1a by overlaying consecutive frames taken at the rate of 10 frames per second. The cell body appeared as a sharp bright spot when it was in the focal plane and as a ring when it was away. Wu *et al.* [9] found that the ring size was proportional to the distance of the cell from the focal plane and therefore can be calibrated to determine the distance. Two examples of 3-D trajectories of the cells 1 and 2 in Fig. 1a are plotted in Figs. 1b and 1c. Most cells approached the surface at an angle and then swam parallel to the surface for some time before leaving. The manner of *C. crescentus* hitting a surface is similar to

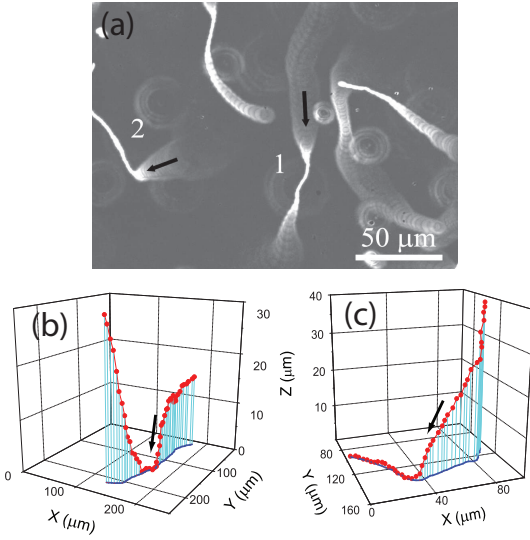


Figure 1: Trajectories of *Caulobacter* swarmer cells swimming near a glass surface. (a) Overlay of consecutive darkfield images taken at 10 frames per second. (b) and (c) are 3-D plots (red) and projections (blue) on the glass surface of the trajectories of cells 1 and 2 in (a). Arrows indicate the swimming directions.

that of *E. coli* observed with three dimensional tracking microscopy [10].

We analyzed the force and torque on *C. crescentus* swimming near a surface and found that it would invariably swim parallel to the surface shortly after hitting the surface. For purposes of the model, we approximate the cell as a sphere attached with a helical filament of length L propelled by a longitudinal force F_p . After the cell hits the surface at an angle θ , its velocity component along the direction normal to the surface (y -axis Fig. 2a) becomes zero. It will have a swimming speed V_x along the x -axis and a rotation rate Ω along the z -axis (not shown in the figure). We ignore the increase in hydrodynamic drag on the cell due to the nearby surface [7, 11] and assume that the surface only provides a force F_s to stop the swimming along the y -axis. The hydrodynamic drag forces on the whole cell (sphere plus helical filament) are split into components parallel and perpendicular to the long axis, F_{\parallel} and F_{\perp} . The hydrodynamic torque Γ on the whole cell is depicted with respect to the sphere center. The forces and torque are given by

$$\begin{pmatrix} F_{\parallel} \\ F_{\perp} \\ \Gamma \end{pmatrix} = \begin{pmatrix} -A_{11} & 0 & 0 \\ 0 & -A_{22} & A_{23} \\ 0 & A_{32} & -A_{33} \end{pmatrix} \begin{pmatrix} V_{\parallel} \\ V_{\perp} \\ \Omega \end{pmatrix} \quad (1)$$

where $V_{\parallel} = V_x \cos \theta$ and $V_{\perp} = V_x \sin \theta$ are the speed components along and perpendicular to the helical axis and A is the friction matrix, where $A_{ij} > 0$ and $A_{23} = A_{32}$.

At a low Reynolds number, the force balance along x -axis is $F_p \cos \theta + F_{\parallel} \cos \theta + F_{\perp} \sin \theta = 0$ and torque balance along z -direction is $\Gamma = 0$, which together determine the

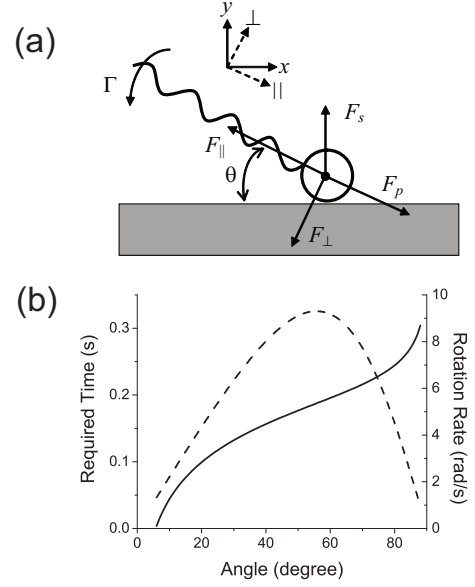


Figure 2: (a) Force and torque analysis of a forward swimming cell hitting a surface. (b) Required time (solid) for the cell to become parallel to the surface and the rotation rate (dashed) as function of angle θ .

swimming speed and rotation rate as

$$V_x = \frac{A_{33} \cos \theta}{A_{33}(A_{11} \cos^2 \theta + A_{22} \sin^2 \theta) - A_{23}^2 \sin^2 \theta} F_p \quad (2)$$

$$\Omega = \frac{A_{23} \sin \theta \cos \theta}{A_{33}(A_{11} \cos^2 \theta + A_{22} \sin^2 \theta) - A_{23}^2 \sin^2 \theta} F_p \quad (3)$$

Since $A_{22}A_{33} > A_{23}^2$, the denominator in the expressions above are always positive. In the case as shown in Fig. 2a, $V_x > 0$ and $\Omega > 0$. Therefore the cell swims toward the right and the filament rotates toward the surface.

We can estimate how fast the cell turns parallel to the surface during the collision. Mathematically, the cell would take an infinitely long time to become parallel to the surface, as calculated from Eq. 3. In practice, however, since the rotational Brownian motion of *C. crescentus* varies its orientation by 0.1 rad within less than 0.1 sec, we estimate instead the time needed for the cell alignment with the surface to fall under 0.1 rad. The parameters for a typical *C. crescentus* [7, 12] are $A_{11} = 2.2 \times 10^{-8}$ Nsm $^{-1}$, $A_{22} = 2.5 \times 10^{-8}$ Nsm $^{-1}$, $A_{33} = 1.9 \times 10^{-19}$ Nms, and $A_{23} = 5.3 \times 10^{-14}$ Ns. The propulsive force is $F_p = A_{11}V \sim 1 \times 10^{-12}$ N, where V is the bulk swimming speed. The rotation rate after hitting a surface is shown in Fig. 2b, which reaches 9 rad/s at 55°. If a cell hits the surface at an angle θ_0 , the time for it to become parallel is $\int_{\theta_0}^{\theta} d\theta / \Omega$ (Fig. 2b). This is less than 0.2 s for a typical angle of $\theta_0 = 30^\circ$, and less than 0.3 s for an angle as large as 85°. Therefore in the following discussion we state in a practical sense that a cell becomes parallel to the surface after the collision.

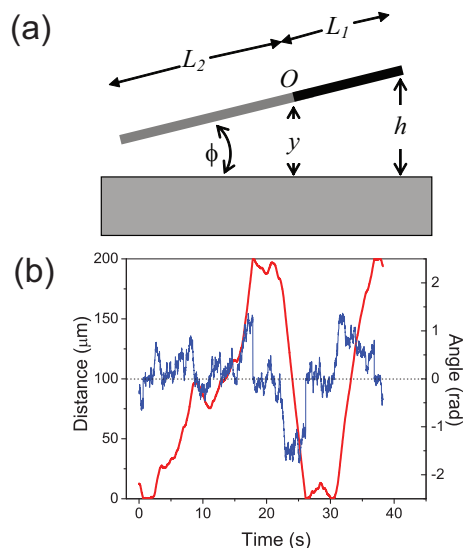


Figure 3: (a) Rod model of a microswimmer near surface. The black end represents that of the cell body and the gray end the flagellar filament. (b) An example of simulated distance h (red) and angle ϕ (blue) as functions of time for the microswimmer, using the parameters of *C. crescentus*. The two surfaces are separated by 200 μm .

Now we examine how a swimming microorganism takes off after hitting a surface. To further simplify the model, we approximate the elongated swimmer propelled by a longitudinal force as a nonuniform rod (Fig. 3a). This rod swims forward at speed V in the bulk fluid. The rod has a rotation center at position O , which is of a distance L_1 away from the head and L_2 away from the tail. The head has a larger drag per unit length than the tail does, and thus $L_1 < L_2$. Due to the small size, the rod undergoes constant Brownian motion with a rotational diffusion constant D_r and translational diffusion constant D_t . Since $A_{11} \sim A_{22}$, we ignore the angle dependence of D_t .

The change in distance of the rotation center to the surface y is determined by the translational Brownian motion and the swimming direction, which is constantly altered by the rotational Brownian motion. Over a time interval Δt , $\Delta y = V \sin \phi \Delta t + \zeta \sqrt{2D_t \Delta t}$, and $\Delta \phi = \zeta \sqrt{2D_r \Delta t}$, where ζ and ζ are random numbers with zero mean and unit variance. The translational Brownian motion contributes much less than swimming to the displacement for microorganisms swimming at tens of $\mu\text{m}/\text{s}$. When near the surface, the changes in distance and angle are also restricted by the solid surface to satisfy $y \geq L_1 \sin(-\phi)$ when the head is closer to the surface and $y \geq L_2 \sin \phi$ when the tail is closer. Similar restrictions hold when a cell is near the top surface. Knowing D_t and D_r , we can track the distance y and angle ϕ over time. The distance of the head from the surface h , which is what was measured in the experiments, is determined by $h = y + L_1 \sin \phi$. The probability distribution of a cell at distance h is obtained by tracking a cell swimming between the two surfaces over $10^6 - 10^7$ sec.

We simulated the distance and angle of swimming *C. crescentus* between two glass surfaces separated by 200 μm . The cell was treated as a $L = 6 \mu\text{m}$ rod, with a typical translational diffusion constant on the order of 0.1 $\mu\text{m}^2/\text{s}$ and the measured rotational diffusion constant of 0.12 rad^2/s . The rotation center was approximated at a position where $L_1 = 0.3L$. Fig. 3b shows examples of distance (red) and angle (blue) varying over time. The cell hits the top and bottom surfaces repeatedly as it swims between them. The simulated distance from the bottom surface was recorded every 0.1 second and a histogram of distances was made using a bin size of 10 μm . The simulated distribution is plotted in Fig. 4 (blue) and compared with the measured one for *C. crescentus* (triangle). The simulation clearly shows higher densities near the surfaces, with the entire profile in excellent agreement with the measurements.

This model is also applicable to the distribution of *E. coli* and bull spermatozoa between two surfaces. We took the cell number distribution of *E. coli* from reference [3] and that of bull spermatozoa from reference [4], converted them to probability density, and plotted them in comparison with that of *C. crescentus* in Fig. 4. *E. coli* is similar in size to *C. crescentus* and it is not surprising that they have similar distributions. Bull spermatozoa are ten times larger yet surprisingly the distribution is similar to that of bacteria. Nevertheless, this similarity is actually predicted by our model. To simulate for bull spermatozoa, we treated it as a 60 μm long rod with a translational diffusion constant on the order of 0.01 $\mu\text{m}^2/\text{s}$ and a rotational diffusion constant of $D_r = 10^{-4} \text{rad}^2/\text{s}$, which is ~ 1000 times smaller than that of *C. crescentus*. The simulation shows that the difference in distribution between the bull spermatozoa (red) and the *C. crescentus* (red) is so small that it cannot be distinguished by the observations under the set conditions.

The distribution of swimming cells near a surface can be understood intuitively based on the variation of angle due to rotational Brownian motion. Once a cell hits a surface, the angle becomes zero and the cell swims parallel to the surface for some time. The cell then swims away from the surface by changing swimming direction due to rotational Brownian motion. Let us examine, for instance, the time t_1 and t_2 needed for a cell to swim to different distances from the surface, $h_1 < h_2$. Since the cell swims to distance h_1 before reaching h_2 , $t_1 < t_2$ must hold. Assuming the swimming direction is only affected by rotational Brownian motion, the mean square angle at time t is $\langle \phi^2 \rangle \sim 2D_r t$. Therefore, the closer a cell swims near the surface, the smaller the angle is. The perpendicular component of swimming speed $V_y = V \sin \phi$ is smaller when closer to the surface. The dwell time of a cell staying at a distance h is inversely proportional to V_y and therefore the probability density is larger near the surface. Additional features of the distribution can be understood based on this physical picture. When the cell swims close to the surface after a collision, $\phi \ll 1$. The probability density is $\sim 1/\phi$, which drops sharply

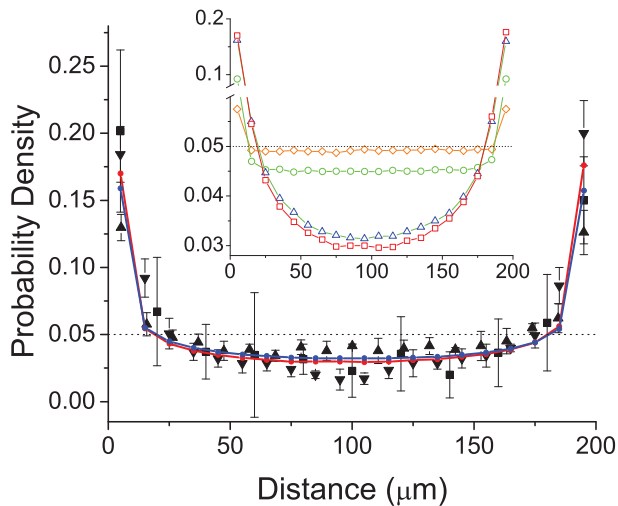


Figure 4: Comparison between simulated density distributions at rotational diffusion constants 0.12 (blue) and 0.0001 (red) rad^2/s and the measured distributions of *C. crescentus* (up triangle), *E. coli* (down triangle, ref [3]), and bull spermatozoa (square, ref [4]). The separation between the two glass surfaces is 200 μm . Inset compares simulated distribution at rotational diffusion constants of 10 (diamond), 1 (circle), 0.1 (triangle), and 0.0001 (square) rad^2/s at a swimming speed of 50 $\mu\text{m}/\text{s}$, corresponding to rod lengths of $\sim 1.3, \sim 2.8, \sim 6,$ and $\sim 60 \mu\text{m}$, respectively. The dotted lines indicate the probability density if there is no surface accumulation.

with the increasing angle and distance. This picture also predicts that a microswimmer with a large rotational diffusion constant leaves a surface more rapidly after a collision and hence the accumulation near the surface is weaker, as shown for $D_r = 10 \text{ rad}^2/\text{s}$ in the inset of Fig. 4.

In this model we have ignored the hydrodynamic interaction between the cell and the surface. In reality, the swimming cell generates a flow, which interacts with the nearby surface, reorienting and attracting the cell towards the surface. Berke *et al.* [3] calculated this effect

for bacteria when the cell is $>10 \mu\text{m}$ away from the surface. A simple estimation shows that this effect is small compared to rotational Brownian motion and swimming when the cell is nearly parallel to the surface. For example, at a distance $h = 10 \mu\text{m}$ and angle $\phi = 0.1 \text{ rad}$, calculation based on their model yields a reorientation rate of $\sim 0.01 \text{ rad}/\text{s}$ and an attraction speed of $\sim 1 \mu\text{m}/\text{s}$, while in 1 second the rotational Brownian motion can reorient the cell by 0.4 rad on average and the component of swimming speed normal to the surface is on the order of 10 $\mu\text{m}/\text{s}$. Therefore, the modification to the distribution due to the long range hydrodynamic interaction is small when the distance is $>10 \mu\text{m}$. When a cell is less than 1 μm from the surface, the large hydrodynamic friction between the cell and surface may keep the cells near the surface for a long time [11]. The effect of this extension of dwell time is not that dramatic since the distribution is binned by 10 μm in distance. The hydrodynamic interaction in the range of 1 to 10 μm is yet to be described theoretically. Its effect on distribution of cells in this range, however, is expected to be secondary as evident by the good agreement between the simulation results ignoring it and the experimental measurements.

In conclusion, we have demonstrated the effects of collision and rotational Brownian motion on swimming microorganisms near surfaces. The collision with a surface resets the swimming direction to be parallel to it and the rotational Brownian motion then randomly alters the swimming direction, which leads to the accumulation. An excellent agreement is obtained between the simulations based on this picture and the experimental results. Recently, various artificial microswimmers have been developed [13, 14, 15], which usually have an elongated shape. Similar effect of the collision and rotational Brownian motion is expected when they swim near a surface.

This work is supported by NIH GM077648 and NSF CMMI 0825873. We thank Professors Y. Brun of Indiana University and B. Ely at University of South Carolina for providing the bacteria strains.

-
- [1] P. Watnick and R. Kolter, *J. Bacteriol.* **182**, 2675 (2000).
 - [2] D. R. Levitan and C. Petersen, *Trends Ecol. Evol.* **10**, 228 (1995).
 - [3] A. P. Berke, L. Turner, H. C. Berg, and E. Lauga, *Phys. Rev. Lett.* **101**, 038102 (2008).
 - [4] L. Rothschild, *Nature* **198**, 1221 (1963).
 - [5] L. J. Fauci and A. McDonald, *Bulletin of Mathematical Biology* **57**, 679 (1995).
 - [6] H. C. Berg, *Random walks in biology* (Princeton University Press, Princeton, 1993), rev. ed.
 - [7] G. Li, L.-K. Tam, and J. X. Tang, *Proc. Nat. Acad. Sci.* **105**, 18355 (2008).
 - [8] S. T. Degnen and A. Newton, *J. Mol. Biol.* **129**, 671 (1972).
 - [9] M. M. Wu, J. W. Roberts, and M. Buckley, *Exp. Fluids* **38**, 461 (2005).
 - [10] P. D. Frymier, R. M. Ford, H. C. Berg, and P. T. Cummings, *Proc. Nat. Acad. Sci. USA* **92**, 6195 (1995).
 - [11] E. Lauga, W. R. DiLuzio, G. M. Whitesides, and H. A. Stone, *Biophys. J.* **90**, 400 (2006).
 - [12] S. Koyasu and Y. Shirakihara, *J. Mol. Biol.* **173**, 125 (1984).
 - [13] R. Dreyfus, J. Baudry, M. L. Roper, M. Fermigier, H. A. Stone, and J. Bibette, *Nature* **437**, 862 (2005).
 - [14] F. Y. Ogrin, P. G. Petrov, and C. P. Winlove, *Phys. Rev. Lett.* **100**, 218102 (2008).
 - [15] P. Dhar, T. M. Fischer, Y. Wang, T. E. Mallouk, W. F. Paxton, and A. Sen, *Nano Lett.* **6**, 66 (2006).